

SALS, a WH2-Domain-Containing Protein, Promotes Sarcomeric Actin Filament Elongation from Pointed Ends during *Drosophila* Muscle Growth

Jianwu Bai,^{1,*} John H. Hartwig,³ and Norbert Perrimon^{1,2,*}

¹Department of Genetics

²Howard Hughes Medical Institute

Harvard Medical School, 77 Avenue Louis Pasteur, Boston, MA 02115, USA

³Hematology Division, Brigham and Women's Hospital, Boston, MA 02115, USA

*Correspondence: jbai@genetics.med.harvard.edu (J.B.), perrimon@receptor.med.harvard.edu (N.P.)

DOI 10.1016/j.devcel.2007.10.003

SUMMARY

Organization of actin filaments into a well-organized sarcomere structure is critical for muscle development and function. However, it is not completely understood how sarcomeric actin/thin filaments attain their stereotyped lengths. In an RNAi screen in *Drosophila* primary muscle cells, we identified a gene, *sarcomere length short* (*sals*), which encodes an actin-binding, WH2 domain-containing protein, required for proper sarcomere size. When *sals* is knocked down by RNAi, primary muscles display thin myofibrils with shortened sarcomeres and increased sarcomere number. Both loss- and gain-of-function analyses indicate that SALS may influence sarcomere lengths by promoting thin-filament lengthening from pointed ends. Furthermore, the complex localization of SALS and other sarcomeric proteins in myofibrils reveals that the full length of thin filaments is achieved in a two-step process, and that SALS is required for the second elongation phase, most likely because it antagonizes the pointed-end capping protein Tropomodulin.

INTRODUCTION

Striated muscles in both insects and vertebrates have remarkably regular and precise organizations that are intimately linked to their function. Sarcomeres, the basic contractile units of myofibrils in muscles, are composed of actin (thin) and myosin (thick) filaments and their associated proteins (Figure 1A). Interestingly, although the length of thin filaments is strikingly uniform within individual sarcomeres, there are significant differences in the absolute length of thin filaments in different muscle types of the same animal (Granzier et al., 1991) as well as in muscles of different species (Page and Huxley, 1963). Furthermore, variations in thin-filament length are believed to be

responsible for the distinct mechanical properties characteristic of each muscle (Burkholder et al., 1994), because the thick-filament length is fairly constant (Page and Huxley, 1963). According to the crossbridge theory of muscle contraction (Huxley and Simmons, 1971), the extent of overlap between thin and thick filaments determines the amount of force that a muscle can exert at different sarcomere lengths. Finally, abnormal thin-filament lengths are thought to be the molecular basis for several debilitating muscle diseases, such as nemaline myopathy and dilated cardiomyopathy (Littlefield and Fowler, 1998; Sussman et al., 1999). Thus, the precise regulation of thin-filament length is critical for muscle function and muscle integrity.

Sarcomeric actin filaments are organized with their two ends lined up in regular arrays (Figure 1A). The barbed (plus) ends are capped by CapZ and are crosslinked by α -actinin at the Z line. Tropomodulin (Tmod), another capping protein, binds to the free pointed (minus) ends located in the middle of the sarcomere toward the H zone, a region free of thin filaments. In nonmuscle cells, it is generally believed that most, if not all, actin assembly is regulated at the barbed ends, and that pointed ends are the sites of disassembly (i.e., treadmill process) (Pollard et al., 2000). Thus, barbed-end and pointed-end capping proteins are thought to influence filament lengths in nonmuscle cells by terminating growth at the barbed ends and by preventing shortening at the pointed ends, respectively (Fischer and Fowler, 2003). In contrast, the length of sarcomeric actin filaments in striated muscles is primarily regulated by modulation of the pointed-end capping activity of Tmod (Fischer and Fowler, 2003). Excess Tmod in striated muscles causes shortening of thin filaments (Littlefield et al., 2001; Mardahl-Dumesnil and Fowler, 2001; Sussman et al., 1998). Conversely, inhibition of Tmod expression or function results in lengthening of thin filaments (Gregorio et al., 1995; Sussman et al., 1998). Thus, unlike capping proteins in nonmuscle cells, which prevent disassembly, Tmod limits actin assembly at the pointed ends of thin filaments. This may be due to the high actin concentration and highly stable actin arrays in muscle tissues. These observations strongly suggest that thin filaments can elongate from pointed ends (Littlefield et al., 2001; Mardahl-Dumesnil and Fowler, 2001; Sussman et al.,

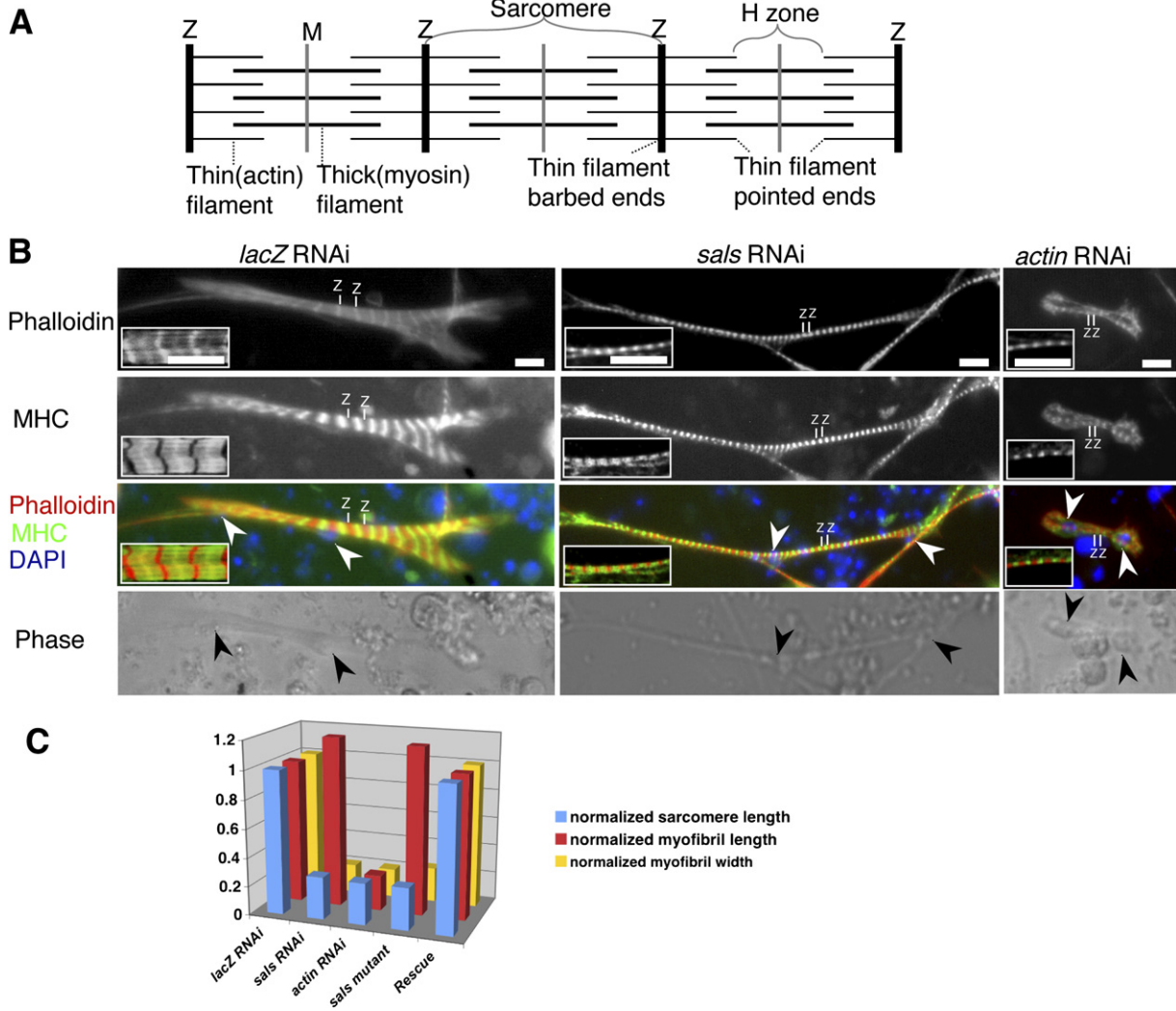


Figure 1. Muscle Defects Caused by dsRNAs Targeting *sals* in Primary Culture

(A) Schematic drawing of a myofibril with three sarcomeres.

(B) Representative fluorescence micrographs of primary muscles derived from myoblasts dissociated from WT embryos and treated with dsRNAs targeting either *lacZ* as WT controls (left panels) or *sals* (middle panels) or *actin* (right panels). Muscles are stained with phalloidin for F-actin (red in merge), an antibody against muscle myosin (MHC) (green in merge), and DAPI for nuclei (blue in merge). The bottom panels are phase images of primary muscles shown in the above panels. Arrowheads point to the nuclei in muscles. The insets are confocal fluorescence images showing the organization of sarcomeres at a higher magnification. The scale bar is 10 μm .

(C) A histogram showing the comparison of primary myofibril features among control *lacZ* RNAi, *sals* RNAi, *actin* RNAi muscles (12 days at 18°C), and those derived from cells isolated from either *sals* homozygous mutant embryos (*sals* mutant) or embryos of *Dmef2-Gal4, sals¹⁰⁷⁸⁴⁹/UAS-sals, sals¹⁰⁷⁸⁴⁹ (Rescue)* (5 days at 25°C). These features include sarcomere length, myofibril length, and myofibril width, all of which are normalized with control *lacZ* RNAi myofibrils. The length of the sarcomeres was determined by measuring the distance between Z lines. The lengths of sarcomeres in myofibrils of *sals* RNAi and *actin* RNAi and the *sals* mutant are $1.77 \pm 0.042 \mu\text{m}$ (average \pm SEM) (range from 1.36 to 2.27 μm), $1.74 \pm 0.08 \mu\text{m}$ (range from 1.30 to 2.38 μm), and $1.70 \pm 0.075 \mu\text{m}$ (range from 1.30 to 2.15 μm), respectively, which are much shorter than the control sarcomere length ($6 \pm 0.73 \mu\text{m}$ [range from 4.56 to 7.9 μm]) and that of *Rescue* myofibrils ($5.5 \pm 0.06 \mu\text{m}$; range from 2.4 to 6.7 μm). The width of myofibrils from both *sals* and *actin* RNAi and the *sals* mutant was $\sim 20\%$ of controls ($p < 0.01$). The width of *Rescue* myofibrils is comparable to that of *lacZ* RNAi controls. Both the lengths of myofibrils and the number of sarcomeres in myofibrils were calculated and normalized by the number of muscle nuclei. The average myofibril length (per nucleus) is $60 \pm 5 \mu\text{m}$ for *sals* RNAi myofibrils, versus $54 \pm 4 \mu\text{m}$ for controls. $n \geq 15$ primary muscles with visual phenotypes scored in each of three independent experiments.

1998). In addition to Tmod, several other proteins are also involved in the regulation of thin-filament length. Tropomyosin (TM) stabilizes thin filaments by copolymerizing with them and by modulating Tmod binding affinity to the

pointed ends (Littlefield and Fowler, 1998). The actin-depolymerizing factor (ADF)/cofilin regulates thin-filament depolymerization from their pointed ends (Mohri et al., 2006), and nebulin may act as a molecular ruler that

dictates thin-filament lengths in vertebrates (Bang et al., 2006; McElhinny et al., 2005; Witt et al., 2006). Despite the fact that the above-mentioned proteins are linked to either capping, stabilization, or depolymerization of thin filaments, the protein(s) responsible for promoting filament elongation remains unknown.

To identify additional regulators of sarcomere assembly, we developed a screening strategy based on RNA interference (RNAi) in *Drosophila* primary muscle cells (J.B. et al., unpublished data). Here, we report the characterization of Sarcomere Length Short (SALS), a novel actin-binding, WH2-containing protein identified by using this approach. Loss of SALS causes shortening of thin filaments and lack of actin incorporation at their pointed ends. Our analyses reveal that SALS promotes thin-filament lengthening from the pointed ends, most likely by antagonizing Tmod capping activity.

RESULTS

Primary Muscle Phenotypes Caused by the Disruption of *sals* by RNAi

Our protocol for RNAi screening in primary muscle cells (see [Experimental Procedures](#)) is based on the ability of cultured myoblasts isolated from *Drosophila* gastrulating embryos (4–6 hr after egg laying [AEL]) to fuse and differentiate into striated muscles in the same sequence of developmental events as observed in vivo (Bernstein et al., 1978). Simply bathing primary cells in medium containing dsRNAs knocks down gene expression in primary muscles (J.B. et al., unpublished data) (Figure 2I).

Using this method, we identified CG31374 (FBgn0051374), which we named “sarcomere length short (*sals*)” based on the striking myofibril phenotypes caused by RNAi. In primary cultures treated with dsRNAs against *sals* (referred to as “*sals* RNAi” in the text), we observed three distinct phenotypes (Figures 1B and 1C). First, *sals* RNAi myofibrils contained much shortened sarcomeres (the lengths of sarcomeres were only ~30% of *lacZ* RNAi controls). Second, these myofibrils were much thinner. These phenotypes were also observed when primary muscles were treated with dsRNAs simultaneously targeting all actin isoforms (referred to as “*actin* RNAi”) (Figures 1B and 1C), which may reflect an arrest in myofibril assembly due to a lack of actin building blocks. Third, *sals* RNAi myofibrils possessed more sarcomeres than controls, with an average of 35 and 9 per nucleus, respectively ($p < 0.001$). Interestingly, the lengths of control versus *sals* RNAi myofibrils were comparable (Figures 1B and 1C). This is in contrast to *actin* RNAi myofibrils, which do not exhibit an increase in sarcomere numbers (~7.5 versus ~9/per nucleus in controls), thus resulting in a shorter myofibril length (Figures 1B and 1C). Finally, *sals* RNAi muscles contained 3.46 ± 0.062 (average \pm SEM) nuclei per fiber, which was comparable to the numbers in controls ($\sim 3.48 \pm 0.5$), suggesting that the phenotype that we observed in *sals* RNAi myofibrils does not result from fewer fusion events.

Molecular Characterization of SALS

sals maps to the cytological position 86E5-86E6 (Figure S1; see the [Supplemental Data](#) available with this article online). It encodes three transcripts, CG31374-RA, CG31374-RB, and CG31374-RC, derived from alternatively spliced RNAs (Figure 2A). CG31374-RA encodes a 497 amino acid (aa) protein (SALS-PA, the short form of SALS), whereas CG31374-RB and CG31374-RC encode the same 899 aa protein (the long form of SALS) (Figure 2B). Both SMART and Pfam searches indicate that the long form of SALS contains two related 10 aa domains (KLRHVACNDR in D1 and KLKPTKTNDR in D2) (Figures 2B and 2C), corresponding to an actin-binding motif known as Wiskott-Aldrich syndrome protein (WASP)-homology domain 2 (WH2). WH2 is a phylogenetically conserved domain found in a variety of proteins from yeast to human, including verprolin, N-WASP, and WIP (Paunola et al., 2002). The SALS long form also contains a profilin-binding proline (Pro)-rich sequence located proximal to the WH2 motifs (Figure 2B). This arrangement is similar to that found in verprolin, N-WASP, and WIP, and it has been proposed to be involved in actin-filament elongation (Chereau et al., 2005). The shorter form, SALS-PA, lacks most of the N terminus of the long form, including the Pro-rich domain and the first WH2 domain (D1).

Whole-mount in situ hybridizations with antisense probes, individually targeting CG31374-RA or CG31374-RB specifically, showed that only the long splice form is expressed during embryogenesis and is restricted to muscles (Figures 2D–2H). Its expression initiates at late stage 13 (Figure 2E) and strengthens from stage 15 onward (Figures 2F and 2G). In addition, only dsRNAs targeting the long *sals* isoform induce muscle phenotypes in primary cultures (Figures 2A and 2I and data not shown). Immunostaining of larval tissues with two different antibodies targeting different regions of SALS (anti-SALS-Bai targets both isoforms, and anti-SALS-Ma [Ma et al., 2006] only targets the long form) revealed that the short form can be found in nonmuscle tissues such as fat body, whereas the long form is only expressed in muscle tissues during larval stages (data not shown).

PBac{WH}f07849 Insertion Produces a Protein Null Allele of *sals*

PBac{WH}f07849, is a piggyBac transposon inserted at the *sals* locus (Thibault et al., 2004). Based on the following evidence, we established that the PBac{WH}f07849 insertion produces a protein null allele of *sals*. First, PBac{WH}f07849 failed to complement *Df(3R)M-Kx1* (86C1; 87B5), a deficiency uncovering *sals*, and both homozygous *sals*^{f07849} mutant embryos and *trans*-heterozygous mutants over a deficiency (*sals*^{f07849}/*Df(3R)M-Kx1*) failed to hatch from the egg case (100% penetrant) and showed similar muscle defects (see below and data not shown). Second, SALS protein (~150 kDa) was not detectable in homozygous *sals*^{f07849} mutants (referred to as “*sals* mutant” below), as measured by immunostaining and by western blot with both anti-SALS antibodies (Figures 2I–2K). Third, remobilization of the piggyBac element

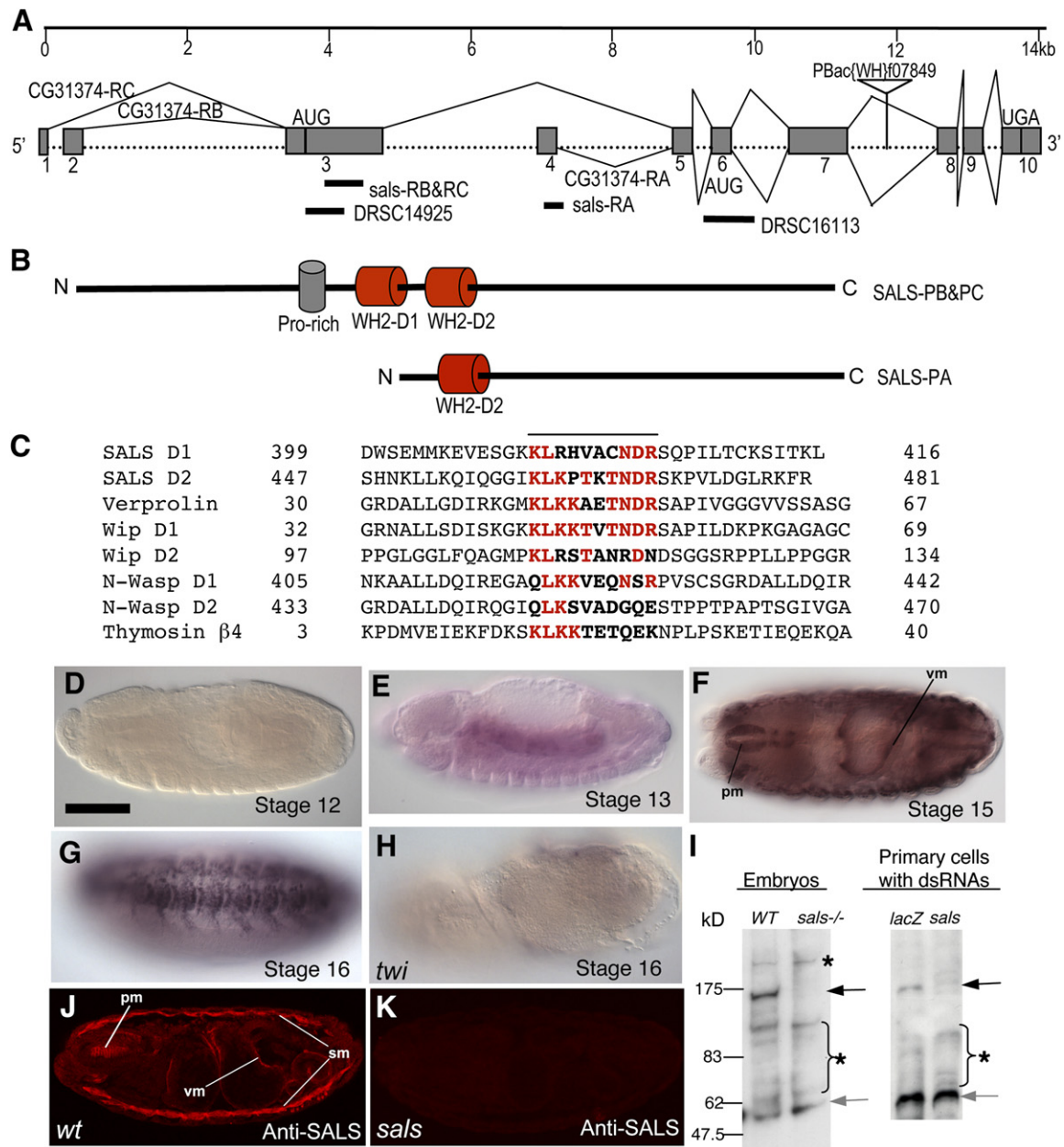


Figure 2. Genomic and Domain Organization, Homology, and Expression of SALS

(A) The *sals* locus spans ~14 kb of genomic DNA. The transcribed regions (gray boxes) and introns (dotted lines) are indicated. The locations of the *sals*¹⁰⁷⁸⁴⁹ piggyBac insertion PBac(WH)07849 and of dsRNAs used to target different SALS isoforms are shown.

(B) Protein structures of the two protein isoforms encoded by the *sals* splice variants.

(C) Alignment of the SALS WH2 domains (bold and underlined) and their flanking sequences with those found in several actin-binding proteins. Amino acids in red indicate conserved ones in the WH2 domain. The D2 domain in the two SALS isoforms displays 53% and 62% sequence identities with the verprolin WH2 domain and the human WIP D1 domain, respectively.

(D–H) Whole-mount embryonic in situ with Dig-labeled antisense probes specifically targeting the long *sals* isoform (anterior is oriented toward the left). (D, E, G, and H) Lateral views. (F) A dorsal view. pm, pharyngeal muscles; vm, visceral muscles that surround the gut; sm, somatic body wall muscles. (D–G) WT embryos. (H) A *twist* (*twi*) mutant embryo showing no *sals* expression. Because *twi* mutant embryos lack mesoderm derivatives, it is confirmed that the long splice form is restricted to muscle tissues.

(I) Western blots probed with rabbit anti-SALS-Ma and mouse anti-tubulin. (Left) Lysates prepared from WT and homozygous (*sals*¹⁰⁷⁸⁴⁹/*sals*¹⁰⁷⁸⁴⁹) larvae (22–24 hr AEL), which were directly ground in SDS sampling buffer. (Right) Lysates of primary cells treated with dsRNAs targeting either the *lacZ* or *sals* long form, after 12 days at 18°C. Anti-SALS-Ma antibody recognizes the SALS protein at ~150 kDa (black arrows) and also cross-reacts with unrelated bands (asterisks) that are detectable in all samples. The gray arrows indicate the location of the tubulin loading control.

(J and K) Fluorescence micrographs of (J) late-stage-16 WT and (K) *sals* mutant embryos stained with the anti-SALS-Bai antibody.

Scale bars are 50 μ m.

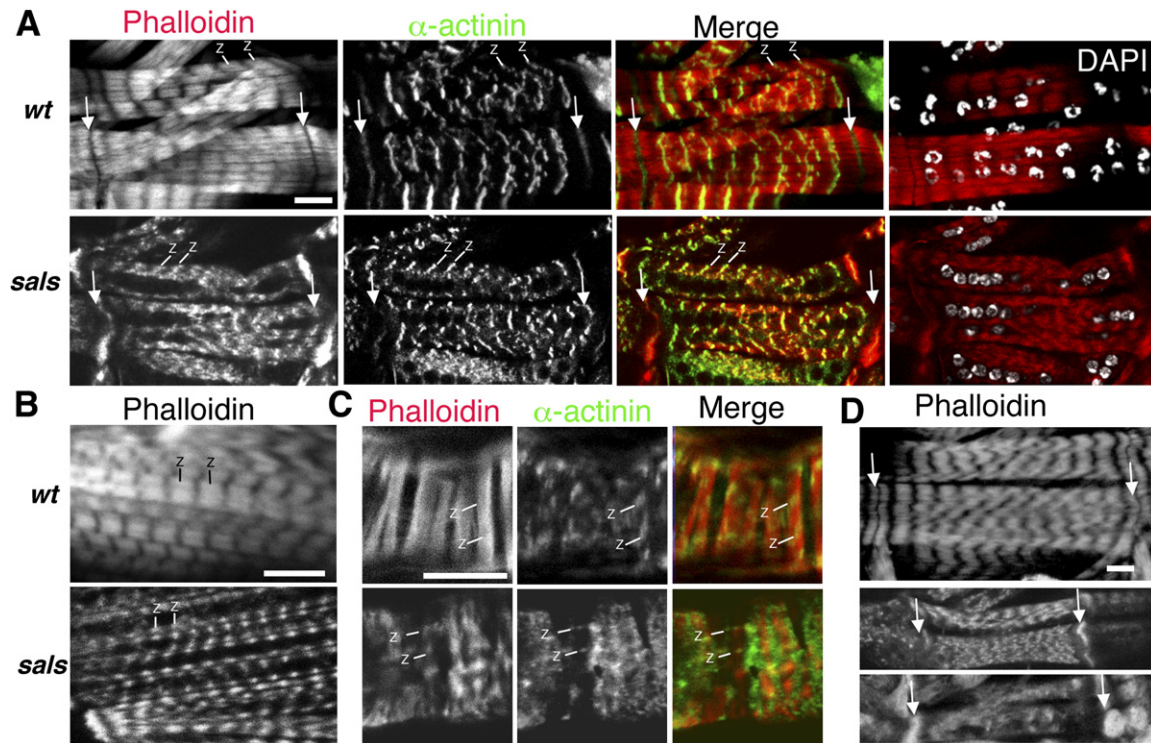


Figure 3. Muscle Defects in *sals* Mutants

(A–C) Confocal fluorescence micrographs of (A) somatic body wall muscles VL3 and VL4, (B) pharyngeal muscle, and (C) visceral muscle from embryos of late stage 17 (19–21 hr AEL), which were visualized for F-actin, for α -actinin, and for nuclei by DAPI staining. The image in the top right panel of (A) shows the same muscles as those in the three top panels on its left, but on a focal plane closer to the muscle periphery. White arrows in (A) point to the termini of muscle VL3. Control sarcomeres in somatic body wall muscle VL3 at A3 averaged $7.7 \pm 0.34 \mu\text{m}$ in length (range from 6.17 to $9.6 \mu\text{m}$, $n = 12$ embryos), whereas *sals*-deficient sarcomeres averaged $5.59 \pm 0.45 \mu\text{m}$ in length (range from 3.4 to $6.9 \mu\text{m}$, $n = 12$) in vivo.

(D) Confocal fluorescence micrographs of somatic body wall muscles VL3 and VL4 from WT larvae (top panel) and posthatching *sals* mutant embryos (bottom two panels) at 28–30 hr AEL, visualized for F-actin.

The scale bars are $10 \mu\text{m}$.

from *PBac{WH}f07849* by using the piggyBac transposase fully rescued the lethality phenotype. Fourth, primary muscles, derived from *sals* mutant embryos, showed similar phenotypes to those associated with *sals* RNAi (Figure 1C). Finally, expression of the long form of SALS in primary muscles by using the muscle Gal4 driver *Dmef2-Gal4* was able to rescue *sals* mutant myofibril phenotypes in primary cultures (Figure 1C).

Muscle Defects in *sals* Mutant Animals

To confirm that the myofibril phenotypes associated with *sals* RNAi in primary muscle cells reflect the function of the gene in vivo, we examined the muscle defects in homozygous *sals*^{f07849} mutants at different developmental stages by using a number of muscle markers. At stage 16, *sals* mutant embryos have normal muscle morphology overall (Figure S2A), and the number of nuclei in mutant muscles is comparable to that in their WT counterparts (Figure S2B), showing that *sals* function is not involved in early critical events of muscle development, such as myoblast specification or fusion. WT muscles do not become mature with well-assembled myofibrils until late stage 17 (19–21 hr AEL) (Newman and Wright, 1981). We therefore

examined the staining patterns of actin and the sarcomere Z line protein α -actinin in somatic body wall, pharyngeal, and visceral gut muscles of late-stage-17 *sals* mutants (Figures 3A–3C). Although myofibrils in both WT and mutant muscles showed striated sarcomeric patterns at this stage, muscles in mutant embryos contained myofibrils with numerous short sarcomeres, a finding analogous to that observed in myofibrils in primary cultures from either *sals* RNAi or *sals* mutant embryos. The primary difference was the degree of reduction in sarcomere length, which was less severe in mutant animals compared to *sals* RNAi muscles grown in culture (~27% reduction versus ~70%) (see Discussion). In addition, whereas WT muscle myofibrils were bundled transversely, mutant myofibrils were thin and split and were distributed along the lateral sides of muscles (Figure 3A). Furthermore, the nuclei in mutant muscles were localized more toward the muscle ends rather than evenly distributed, as observed for nuclei in WT muscles (Figure 3A; see Figure S3 and its legend).

We further examined the muscle structure of “post-hatched” *sals* mutants. WT larval somatic muscles at 28–30 hr AEL displayed a well-organized myofibril structure, and they were still growing longitudinally, as

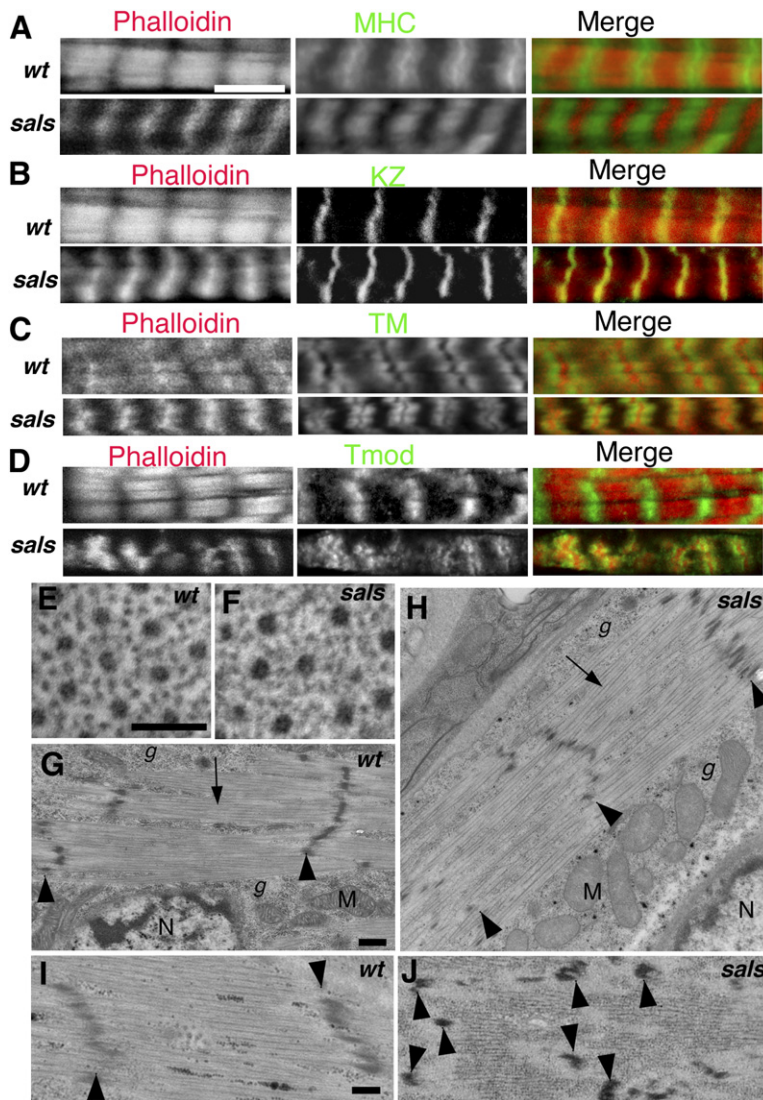


Figure 4. Examination of Myofibril Morphology and Sarcomeric Organization in *sals* Mutant Muscles by Confocal Analysis and Electron Microscopy

(A–D) Confocal micrographs of myofibrils from WT (upper panels) and *sals* mutant embryos (bottom panels) at 20–22 hr AEL. The left panels show F-actin. The middle panels show the stainings for different sarcomeric components: (A) MHC for thick filaments; (B) KZ for SLS in Z lines; (C) TM; and (D) Tmod. The right panels show merged images from the left and middle panels. Note the strong phalloidin stainings at Z lines, and shorter thin-filament and sarcomere lengths in *sals* mutant myofibrils than those in WT, as revealed by phalloidin, TM, and Tmod stainings.

(E–J) (E–H) Electron micrographs of larval muscles from (E, G, and I) WT (w^{1118}) and (F, H, and J) the *sals* mutant ($sals^{107849}/sals^{107849}$) at stages of (E–H) 20–22 hr AEL or (I and J) 28–30 hr AEL. (E and F) Transverse sections at a higher magnification show that the basic contractile unit of a thick filament (large black dots) surrounded by an array of thin filaments (small dots) can form correctly in both (E) WT and (F) *sals* mutant myofibrils. Longitudinal sections of (G) WT muscles and (H) muscles of some mutant embryos ($n = 10$) show regular, parallel, highly ordered arrays of myofilaments with apparent interdigitating thin and thick filaments (arrows) and well-organized Z lines (arrowheads) that are characteristic of larval muscles. Sarcomeres are in a contracted state in both (G) and (H), and they are $\sim 4.5 \mu\text{m}$ and $\sim 3.2 \mu\text{m}$ long, respectively. Glycogen granules (g), mitochondria (M), and nuclei (N) are also labeled in (G) and (H). (I and J) Sarcomeric regions in muscles of an (I) older WT and (J) mutant embryos (28–30 hr AEL). (J) Note that mutants contain electron-dense structures (black arrowheads), and their myofibrillar architecture was severely disrupted.

The scale bar is 10 μm in (A) for (A)–(D), 100 nm in (E) for (E) and (F), 500 nm in (G) for (G) and (H), and 500 nm in (I) for (I) and (J).

evidenced by the increased number of sarcomeres in myofibrils (12 compared to 8 at 19–21 hr AEL) (upper panel in Figure 3D). In contrast, the muscles of age-matched *sals* mutant larvae had many more sarcomeres (~ 18 compared to 12 in controls at 28–30 hr AEL), but they were much shorter in length longitudinally (only $\sim 70\%$ of their WT counterparts) (middle panel of Figure 3D), indicating that the growth rate of *sals* mutant muscles is much slower than that of WT. In addition, some muscles showed a complete disruption of myofibril morphology (bottom panel in Figure 3D) (see Discussion). This extreme phenotype was also evident under an electron microscopy (EM) analysis (Figures 4I and 4J). Interestingly, the numerous electron-dense patches seen under EM (arrowheads in Figure 4J) resemble the condensed thin filaments in conjunction with Z line materials seen in nemaline myopathy (Yamaguchi et al., 1978).

Because *sals* mutants failed to hatch from the egg case, we tested whether this was a result of their inability to move. Peristaltic movement, a characteristic behavior observed before hatching, was detectable in mutant embryos at late stage 17 (20–22 hr AEL at 25°C) (Movie S2). However, compared to control embryos, which exhibit well-coordinated waves of strong forward and backward peristalsis (Movie S1), *sals* mutants had less frequent backward peristalsis, and the vigor of their contraction was much reduced (Figure S4; Movie S2). At 28–30 hr AEL, which was beyond the expected hatch time, mutants displayed weak movements (Movie S3). They eventually died in the egg case within a day. When mutant animals were released from their egg case by manual dissection, they were flaccid and immobile. We conclude that although *sals* mutant embryos can move, they cannot generate sufficient contractile force to escape

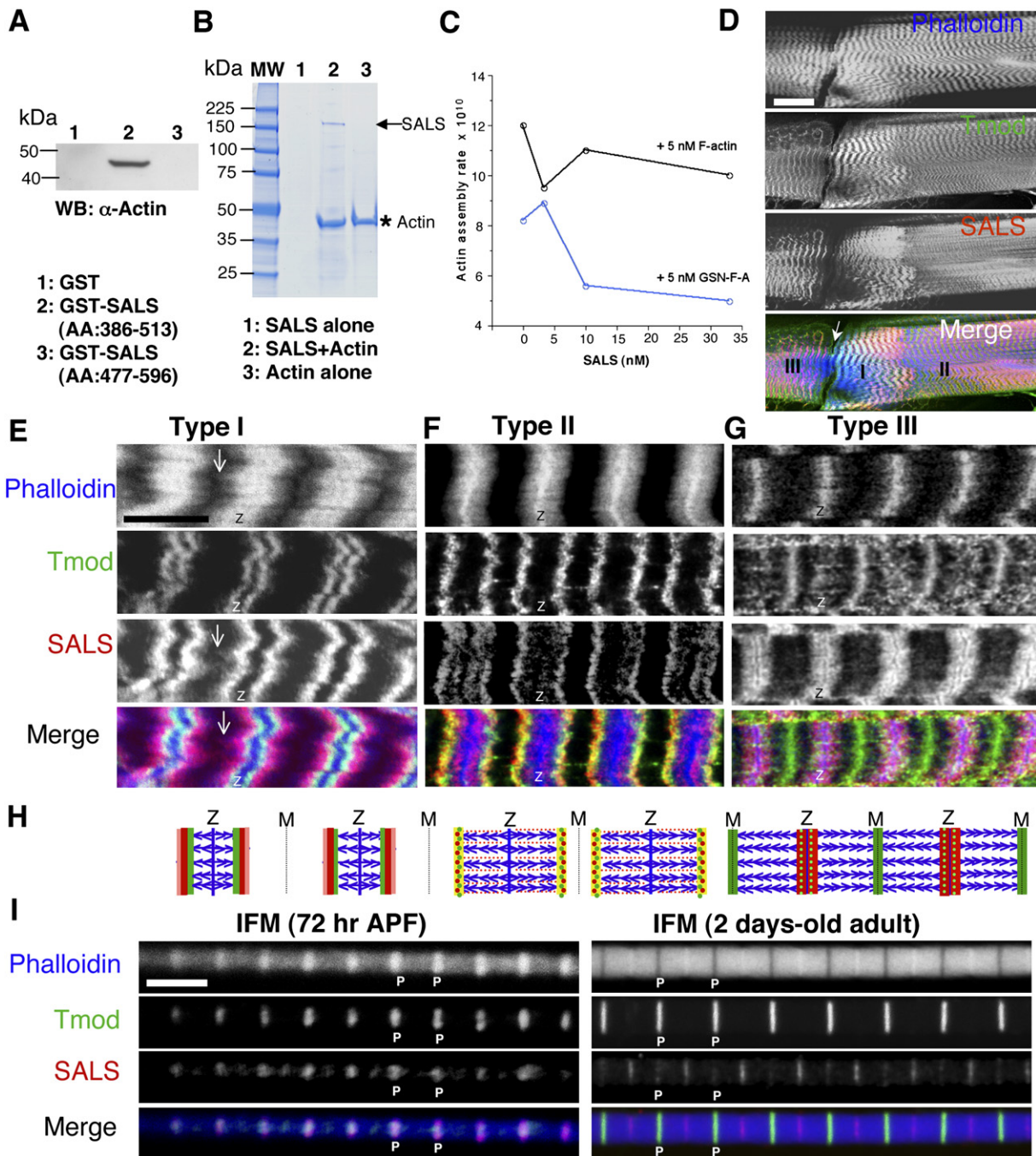


Figure 5. SALS Interacts with Actin and Has a Complex Localization in Myofibrils

(A) GST pull-down assays for interactions between SALS and actin. Equal amounts of proteins derived from the indicated GST and GST-SALS constructs ($\sim 10 \mu\text{g}$) were incubated with $0.05 \mu\text{M}$ G-actin.

(B) Cosedimentation assays of SALS binding to gelsolin-capped F-actin. Purified, recombinant full-length SALS (black arrow) cosedimented with F-actin (asterisk) (lane 2), but not by itself (lane 1).

(C) Effect of recombinant SALS on nucleated actin assembly. Rabbit skeletal muscle actin was polymerized in the absence or presence of human plasma gelsolin (GSN) at a ratio of 1 GSN:50 actin monomers. A total of 5 nM filaments was mixed with SALS protein at different concentrations, and the rate of actin assembly was followed by the addition of $1 \mu\text{M}$ pyrene actin.

(D–G) Representative confocal micrographs of myofibrils in the late-L2 muscle VL3 in A3 fluorescently labeled by phalloidin (blue in merge), Tmod (green in merge), and SALS (red in merge) staining. Z shows the location of the Z line. (D) A confocal micrograph showing two adjacent muscles with at least three different patterns of thin-filament morphology at different locations in the muscle. Type I and III patterns are near muscle termini, and type II is more interior to type I. The arrow points to the muscle termini. (E) Sarcomeres with irregular thin-filament lengths (Type I). Some

from the egg case because of their underlying muscle defects.

***sals* Mutant Sarcomeres Have Short Thin Filaments**

To investigate the organization of sarcomeres in *sals* mutant muscle myofibrils, we dissected WT and *sals* mutants at 19–21 hr AEL, and stained muscles with phalloidin as well as antibodies targeting a number of sarcomeric markers (Figures 4A–4D). These include *Drosophila* muscle Myosin Heavy Chain (MHC) (Figure 4A); KZ, an isoform of the *Drosophila* Titin homolog Sallimus (SLS) localized at the Z line (Machado et al., 1998) (Figure 4B); Tropomyosin (TM) (Figure 4C); and Tmod (Figure 4D).

The overall distribution of these sarcomeric components, except Tmod, appeared to be unaltered in the *sals*-deficient myofibrils (Figures 4A–4D). Whereas Tmod staining was found in or close to the M line of the sarcomere in WT myofibrils, its distribution was very close to the Z line in mutants (Figure 4D). Furthermore, the length of thin filaments was much shorter in mutant sarcomeres ($\sim 0.85 \pm 0.021 \mu\text{m}$ versus $\sim 2.75 \pm 0.086 \mu\text{m}$ [range from 1.8 to 3.4 μm] in WT; myofibrils in body wall muscle VL3 in A3 or A4 were analyzed; $n \geq 12$). The reduced size of thin-filament lengths found in mutant myofibrils was very similar to that of *sals*-deficient myofibrils in primary culture (data not shown). Short thin-filament lengths were independently confirmed by phalloidin staining for F-actin (Figure 3) and by staining for TM (Figure 4C). Notably, the width of MHC staining in mutant myofibrils, although slightly shorter, was comparable to that in WT (Figure 4A), suggesting that the thick-filament length was not dramatically reduced. Altogether, these results indicate that SALS is not critical for the normal organization of several sarcomeric proteins, but that it is essential for achieving the final thin-filament length. This conclusion was further supported by an EM analysis of *sals* mutant muscles, which had well-organized myofibril structures at 20–22 hr AEL, as revealed in both transverse and longitudinal EM sections (Figures 4E–4H).

SALS Binds Both G-Actin and F-Actin and Associates with Filament Pointed Ends

As SALS (referred to as “the long form of SALS” in the text below) has a predicted actin-binding domain, we determined whether it could bind actin. We first examined whether SALS could directly bind to G-actin *in vitro*. Because the full-length GST-SALS protein is not expressed well, we tested two complementary fusion proteins, SALS(386–513) and SALS(477–596), in a pull-down assay.

SALS(386–513), which contains the two WH2 domains, bound G-actin, whereas SALS(477–596), which lacks the WH2 domains, did not (Figure 5A). This suggests that the WH2 domains of SALS are sufficient for G-actin binding.

We further evaluated the capacity of SALS to bind to actin filaments (F-actin) by using a cosedimentation assay. The purified recombinant SALS protein by itself did not sediment at $200,000 \times g$ (30 min). However, SALS cosedimented with gelsolin-capped F-actin (Figure 5B), indicating that SALS binds F-actin through the pointed ends and/or sides, but not through the barbed ends, which were capped by gelsolin in the assay (Yin et al., 1981). The association of SALS with F-actin is specific, because the control protein GST failed to sediment with F-actin (data not shown).

To investigate SALS pointed-end effects, we determined whether it affected actin elongation from gelsolin-capped actin filaments. As shown in Figure 5C, we found that SALS markedly slowed the rate of addition of actin subunits at the pointed end of these capped, but not uncapped, filaments. The effect was observed at a stoichiometry that also eliminates monomer sequestration as a mechanism of diminished pointed-end assembly. Altogether, our data suggest that SALS is associated with the filament pointed ends.

SALS Protein Is Enriched at Pointed Ends during Thin-Filament Elongation

To further characterize the role of SALS in sarcomere elongation, we examined its localization pattern in muscles by using two antibodies targeting two different regions of SALS. Both antibodies showed an identical staining pattern in muscles, and this pattern revealed that SALS is specifically associated with thin filaments, but not with thick filaments (data not shown). Because new sarcomeres are constantly added to myofibrils during muscle growth through three larval stages (L1, L2, L3) (Haas, 1950), we examined SALS localization in late-L2 or early-L3 muscles because they are more easily prepared for visualization.

We investigated the SALS localization pattern with respect to F-actin (by phalloidin staining) and Tmod (Figures 5D–5G), as well as to α -actinin (Figure S5) in somatic body wall muscles. We detected a large variation in thin-filament morphology among different sarcomeres within the same myofibril, although the lengths of these sarcomeres were relatively uniform (Figures 5D–5G). Phalloidin has been reported to have less accessibility to more organized thin filaments, due to their association with actin-binding

thin-filament pointed ends protrude out, forming ragged ends toward the middle of the sarcomere (arrows). (F) Sarcomeres with a more uniform organization of actin filaments (Type II). (G) Sarcomeres with Tmod strongly localized in the M line and SALS preferentially found near the Z line (Type III). (H) Schematic drawing showing the complex distributions of SALS (in red or light red) and Tmod (in green) relative to thin filaments (in blue), based on the confocal micrographs shown in (E)–(G), during thin-filament assembly. Yellow indicates the merge of SALS and Tmod. The black, dotted, thin line: M line; blue thin line: Z line. To simplify, thick filaments are not shown in sarcomeres.

(I) Confocal micrographs of isolated IFM myofibrils from pupae 72 hr APF (left panels) and 2-day-old adults (right panels) fluorescently labeled by phalloidin (blue in merge) and stained for Tmod (green in merge) and SALS (red in merge). P, pointed ends. The scale bar is 50 μm in (D), 10 μm in (E) for (E)–(G), and 5 μm in (I).

proteins such as nebulin, which may block phalloidin from binding to F-actin (Zhukarev et al., 1997). Thus, we determined the level of organization of thin filaments in sarcomeres based on the phalloidin staining pattern: those with broad, fuzzy staining were the least organized (top panels in Figures 5E and 5F), and those with strong, Z line staining were the most organized and usually had the longest length, with their pointed ends meeting in the middle of the sarcomere as a discrete band (Figure 5G). Interestingly, sarcomeres with less organized thin-filament morphology were often detected at the muscle termini (Figures 5D and 5E), where growth is known to take place in vertebrate muscles (Dix and Eisenberg, 1990; Williams and Goldspink, 1971). By analogy, we presume that such sarcomeres represent newly formed sarcomeres, whereas those with a more organized thin-filament morphology are older and full-grown sarcomeres.

The distribution of α -actinin, a marker for thin-filament barbed ends at the Z line, was always located in the midline of the phalloidin staining (Figure S5), confirming that thin filaments are relatively stable at the barbed ends (Littlefield et al., 2001). In contrast, several patterns of Tmod and SALS localization could be distinguished and correlated with the morphology of thin filaments in sarcomeres (middle panels in Figures 5E–5G). Importantly, SALS was localized at the pointed ends of thin filaments while they were elongating (Figures 5E, 5F, and 5H), but it disappeared from the pointed ends of full-grown thin filaments and relocated at the region flanking the Z line, where the fuzzy Tmod staining pattern was also observed [Figures 5G and 5H]. This doublet pattern was more obvious in myofibrils of visceral muscles of third-instar larvae (Figure S5B). A similar distribution pattern has also been observed previously for MLP (Muscle LIM protein), a protein implicated in myofibril growth (Arber et al., 1997). Because *sals*-deficient muscles also have thin myofibrils, we speculate that this doublet pattern flanking the Z lines may represent the sites at which newly assembled thin filaments are located, which may also contribute to the transverse growth of myofibrils. Notably, Tmod distribution was not found at the tip of thin-filament ends in, presumably, newly added sarcomeres, but these were the loci at which the strong SALS staining was observed (arrows in Figure 5E). Thus, we speculate that these ends may not be capped strongly by Tmod while they are still actively elongating, most likely through SALS activity.

Importantly, SALS is also expressed in the adult fly indirect flight muscles (IFM) (Figure 5I). The IFM increase their size by the synchronous lengthening of sarcomeres (from $\sim 1.7 \mu\text{m}$ to $3.2 \mu\text{m}$), whereas the sarcomere number remains unchanged in myofibrils (Reedy and Beall, 1993). This is unlike larval muscles, which grow by increasing sarcomere number through the addition of newly assembled sarcomeres to the existing myofibrils. Thus, IFM provide a better system by which to correlate the positions of SALS to the growth of thin filaments. Indeed, we observed strong localization of SALS at the pointed ends when the thin filaments were still elongating along with sarcomere lengthening in the IFM 72 hr after pupal formation (APF)

(Figure 5I). Furthermore, SALS is less enriched at the pointed ends when thin filaments reach their maximum length, because sarcomere lengthening stops in the IFM of 2-day-old adults (Figure 5I). Altogether, the distribution of SALS in both larval muscles and adult IFM suggests that SALS may be involved in thin-filament elongation from the pointed ends.

SALS Is Required for GFPactin Incorporation at Pointed Ends

To provide further support for the pointed-end activity of SALS, we established primary cell cultures from myoblasts isolated from embryos carrying the *Dmef2-Gal4*, *UAS-GFPactin* transgenes. In these cells, GFPactin was expressed at the stage at which myofibril assembly just starts to occur. This unique timing of expression causes the initial incorporation of GFPactin into thin filaments to be found at both the Z line and the filament pointed ends, either in primary muscles cultured within 5 days at 18°C or in early-L1 muscles (Figure 6A and data not shown). This is consistent with the report from Littlefield et al. (2001) that states that G-actin can be incorporated into both barbed and pointed thin-filament ends. However, after an extended period of culture, either in vivo (such as in third-instar larval muscles) or in primary culture (such as those cultured for 12 days at 18°C), GFPactin was found throughout the entire thin filaments, presumably due to turnover of non-GFP-labeled, endogenous actins and further incorporation of GFPactin (Roper et al., 2005; data not shown). We thus only examined the effects of dsRNAs targeting *lacZ* or *sals* on the initial sites of incorporation of GFPactin in the thin filaments of primary muscles cultured within 5 days at 18°C .

Muscles in primary cultures treated with control *lacZ* dsRNA were similar to muscles in untreated cultures, and, in both cases, the majority displayed two incorporation sites for GFPactin (Figures 6A and 6C): one site colocalized with α -actinin at the Z line, where thin-filament barbed ends are located; the other site mapped to the middle of the sarcomere, at the thin-filament pointed ends. Unlike control primary muscles, the majority of *sals* RNAi primary muscles showed GFPactin incorporation only at the Z lines, with no incorporation at the pointed ends (Figures 6B and 6C). These data strongly indicate that SALS is required for GFPactin incorporation into pointed ends, but not barbed ends.

Converse Effect of SALS and Tmod on Thin-Filament Assembly

Given the decreased length of thin filaments observed in the absence of a functional SALS protein, we tested whether its overexpression could lead to a corresponding increase in thin-filament length. Constitutive expression of SALS in muscles disrupted their function, and 65% of embryos carrying *Dmef2-Gal4*, *UAS-sals* failed to hatch at 29°C ($n = 200$). The remaining, although able to hatch, crawled very slowly and later died. To obviate any complications resulting from the mechanical stress placed by

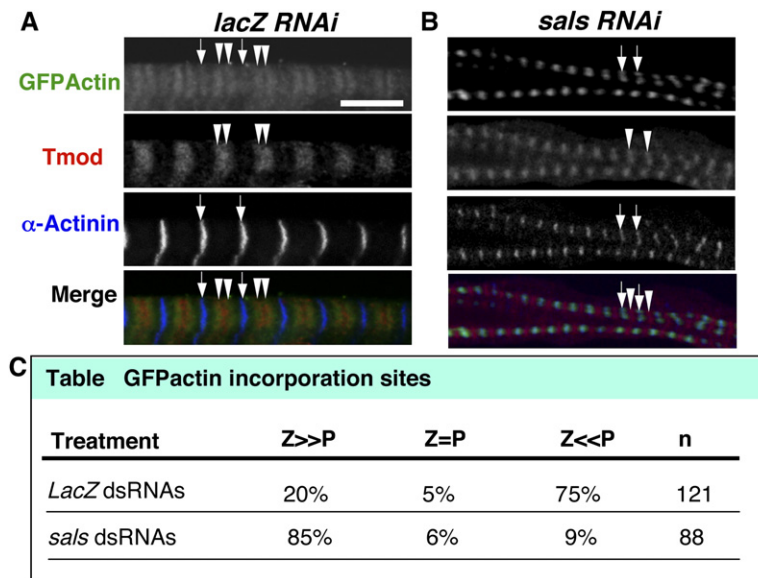


Figure 6. SALS Is Required for GFPactin Incorporation at Pointed Ends

(A and B) Confocal micrographs of primary muscles cultured at 18°C for 5 days, derived from embryos carrying *Dmef2-Gal4/UAS-GFPactin57B*, treated with dsRNAs targeting either (A) *lacZ* or (B) *sals*, visualized by GFP for GFPactin (green in merge), and stained for Tmod (red in merge) and for α -actinin (blue in merge). Arrows, Z lines; arrowheads, pointed ends.

(C) GFPactin incorporation sites. Visual scoring of GFPactin incorporation sites in primary muscles treated with dsRNAs targeting *lacZ* or *sals*. Z>>P, cells in which GFPactin fluorescence was much brighter at Z lines than at pointed ends; Z = P, cells in which GFPactin fluorescence at Z lines and at pointed ends was of approximately equivalent brightness; Z<<P, cells in which GFPactin fluorescence was much dimmer at Z lines than at pointed ends; n, number of primary muscle cells counted.

The scale bar is 10 μ m in (A) for (A) and (B).

other tissues on muscles in vivo, we examined muscle phenotypes in primary culture.

Primary muscle cells isolated from *Dmef2-Gal4, UAS-sals* embryos were cultured for 5 days at 29°C, fixed, and stained with phalloidin and the sarcomeric marker KZ. Strikingly, ~90% of the primary muscles (n = 57) had completely lost the stereotypical striated pattern of thin and thick filaments (Figure 7B). This phenotype was reminiscent of that observed in primary muscles treated with a dsRNA against Tmod (Figure 7A; ~80% penetrant, n = 40), suggesting that excess SALS or loss of Tmod may disrupt initial myofibril assembly (as indicated in the model shown in Figure 7J). However, a small percentage of muscles with excess SALS (~7%, n = 56) contained myofibrils with an aberrant striated pattern with longer than usual sarcomeres (Figure 7E), a phenotype that also could be found in Tmod dsRNA-treated primary myofibrils (~5% penetrant) (Figure 7D), but never found in controls (Figure 7C). These mild phenotypes may reflect a relatively lower level of SALS expression or a partial reduction of Tmod level caused by RNAi in muscle cells, respectively. In the myofibrils containing elongated sarcomeres, staining for KZ or phalloidin revealed a relatively normal, striated Z line pattern, although localization of KZ was slightly altered (middle panels in Figures 7C–7E). However, the staining for Tmod in the primary muscles with either Tmod RNAi or overexpression of SALS was diffuse and did not exhibit any regular striated pattern, as seen in controls (data not shown). Controls had a clear and discrete phalloidin staining band in the middle of the sarcomere, whereas phalloidin staining in the middle of these lengthened sarcomeres was fuzzy and irregular (Figures 7C–7E), showing that their thin filaments are misaligned and have variable lengths, and that some extend across the M line, resulting in no obvious H zone. This observation indicates that excess SALS can cause thin filaments to elongate from the pointed ends.

The antagonistic activities of SALS and Tmod suggest that they might genetically interact in the thin-filament assembly process. To document this interaction, we first confirmed that excess Tmod would result in short thin-filament lengths in primary cultured muscles ($1.8 \pm 0.042 \mu\text{m}$ versus $2.5 \pm 0.034 \mu\text{m}$ in controls; average \pm SD, n \geq 15 primary muscles scored for each genotype), as previously reported to be the case in vertebrate muscles and in fly IFM (Littlefield et al., 2001; Mardahl-Dumesnil and Fowler, 2001) (Figures 7G and 7H). In addition, animals overexpressing Tmod had much higher mortality rates at both embryonic and larval stages compared to the control animals carrying *Dmef2-Gal4* alone (Figure 7F), due to muscle defects resulting from short thin-filament lengths (data not shown). Importantly, reduction of the SALS level enhanced the effect caused by Tmod overexpression, as demonstrated by an increase in embryonic mortality rate (Figure 7F) and a greater reduction in thin-filament lengths in cultured muscles (Figures 7G–7I). Thus, we conclude that Tmod and SALS functionally antagonize each other in thin-filament assembly at the filament pointed ends.

DISCUSSION

SALS Promotes Thin-Filament Elongation from Pointed Ends In Vivo

In this study, we report the characterization of SALS, an actin-binding, WH2-domain-containing protein that is essential for the development and function of *Drosophila* larval muscles. Importantly, we show that SALS is required for the elongation of thin filaments from pointed ends to attain their final lengths in sarcomeres. These conclusions are based on the findings that (1) inactivation of SALS by either RNAi or genetic disruption leads to myofibrils containing shortened thin filaments, (2) the localization of SALS at the filament pointed ends coincides with the growth of thin filaments, (3) GFPactin fails to incorporate

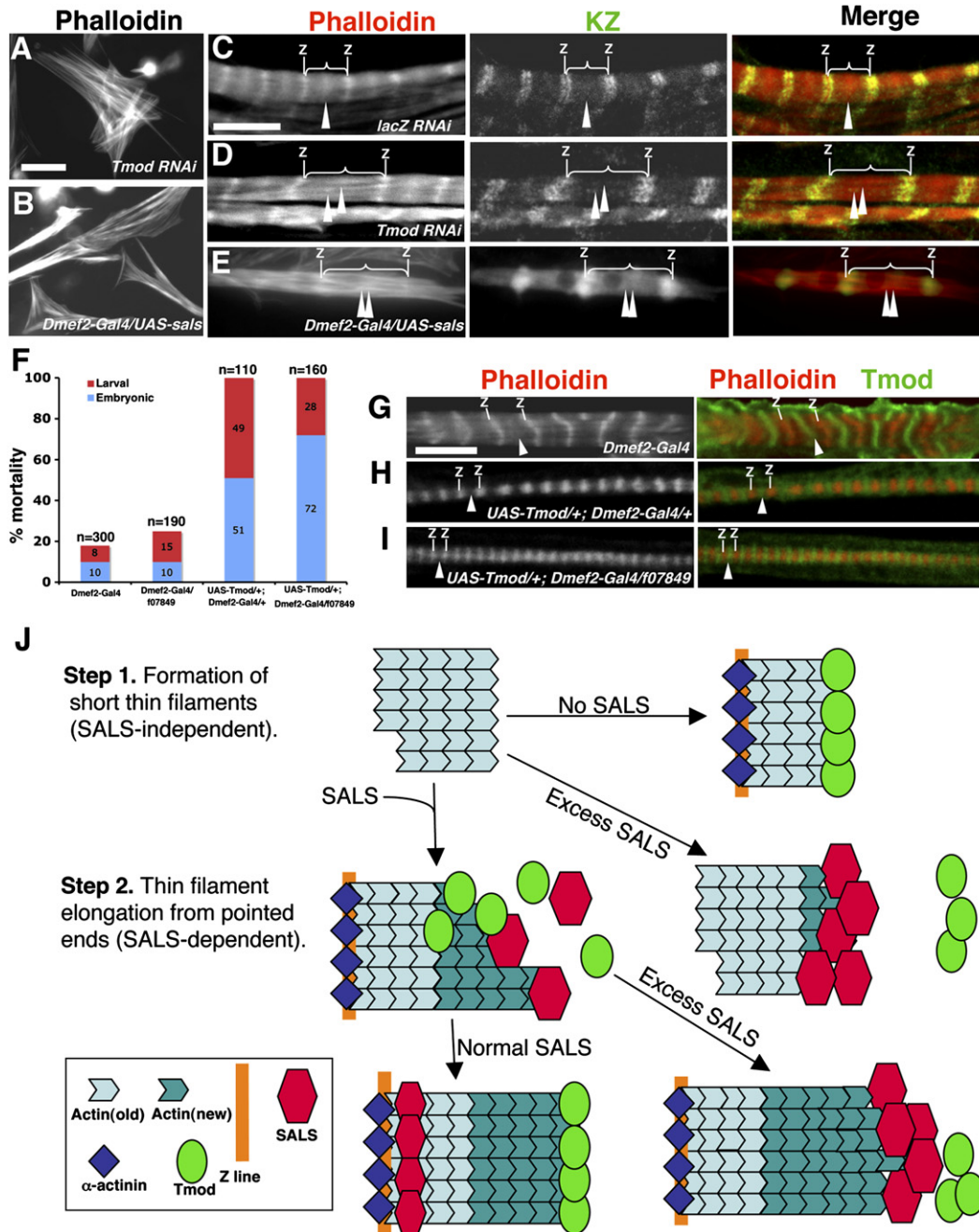


Figure 7. Antagonistic Relationship between SALS and Tmod

(A and B) Fluorescence micrographs of primary muscles visualized by phalloidin. (A) Primary muscles were treated with a dsRNA targeting Tmod. (B) Primary muscles were derived from fly embryos carrying *Dmef2-Gal4, UAS-sals*.

(C–E) Confocal micrographs of primary myofibrils stained by phalloidin (red in merge) and by anti-KZ antibodies for Z lines (green in merge). (C) Control myofibrils treated with *lacZ* dsRNAs. Filament pointed ends joined at the midline of the sarcomere (arrowheads). (D) Myofibrils treated with Tmod dsRNA. (E) Myofibrils derived from embryonic cells carrying *Dmef2-Gal4, UAS-sals*. Note the irregular sarcomere lengths in (D) and (E) compared to those in (C) (white brackets). The white arrowheads in (D) and (E) point to nonuniform pointed ends of thin filaments, compared to the arrowheads in (C).

(F) Mortality rate of animals of different genotypes at embryonic and larval stages.

(G–I) Confocal fluorescence micrographs of primary myofibrils derived from cells isolated from embryos of (G) *Dmef2-Gal4*, (H) *UAS-Tmod/+; Dmef2-Gal4/+*, and (I) *UAS-Tmod/+; Dmef2-Gal4/sals¹⁰⁷⁸⁴⁹*, visualized by phalloidin (red in merge) and Tmod (green in merge). White lines, Z lines; white arrowheads, pointed ends. Note that the average length of thin filaments in *UAS-Tmod/+; Dmef2-Gal4/sals¹⁰⁷⁸⁴⁹* primary muscle myofibrils was ~10% shorter than that found in *UAS-Tmod/+; Dmef2-Gal4/+* primary muscles ($1.6 \pm 0.079 \mu\text{m}$ versus $1.8 \pm 0.042 \mu\text{m}$; average \pm SD, $n \geq 15$).

into thin filaments through pointed ends in the absence of SALS, and (4) SALS overexpression is sufficient to cause overgrowth of thin filaments.

The discovery of SALS is significant because it demonstrates the existence of a protein that appears to promote thin-filament elongation from pointed ends *in vivo*. Our genetic analyses suggest that SALS may act by antagonizing Tmod pointed-end capping activity (Figure 7J). The antagonism may resemble that observed between Ena/VASP proteins and the capping protein (Bear et al., 2002) or between formins and the capping protein (Zigmond et al., 2003) at the barbed end. Loss of SALS would allow Tmod to cap the pointed ends permanently. This is equivalent to the effect of an increase in Tmod levels during myofibril assembly, which converts Tmod from a dynamic to a permanent cap by outcompeting SALS at the pointed end and by preventing SALS from elongating actin filaments. Conversely, overexpression of SALS leads to a phenotype similar to loss of Tmod, because excess SALS might act as an “anticapping” protein to compete with and antagonize Tmod access to the filament pointed ends. Finally, the complex localization patterns of Tmod and SALS, together with their antagonistic relationships, is suggestive of the mechanism deployed during normal thin-filament assembly. Indeed, rapid actin assembly at the uncapped filament pointed ends is consistent with the localization of Tmod that lags behind SALS (Figure 5).

As a protein that binds both G-actin and F-actin, SALS may function by stabilizing F-actin and/or through the direct involvement of actin polymerization. To our surprise, although it is strongly associated with the pointed ends, SALS alone appears to inhibit filament elongation *in vitro* (Figure 5), instead of promoting elongation, as supported by all of the *in vivo* data. This discrepancy may imply that other factors such as Tmod, TM, and profilin-actin are needed in the biochemistry assay to observe the effect of SALS *in vitro*. Indeed, the long form of SALS contains Pro-rich profilin-binding sequences positioned immediately N-terminal to the two tandem actin-binding WH2 domains. Moreover, crystal structure analysis suggests that the Pro-rich regions preceding WH2 domains may facilitate actin-filament elongation by increasing the local concentration of profilin-actin, or that they may mediate actin monomer transfer directly to WH2 via profilin (Chereau et al., 2005).

How Does Lack of SALS Lead to Shortened Sarcomere Length and Increased Sarcomere Number in Myofibrils?

Our analysis of *sals* mutant muscles suggests that the “short sarcomere” phenotype is a consequence of shortened thin filaments. This model is consistent with previous findings that reduced sarcomere lengths are found in

muscles with altered expressions of proteins known to be involved in the regulation of actin-filament lengths, for instance when Tmod is present in excess (Susman et al., 1999). Furthermore, we propose that sarcomere length may be specified during assembly in order to achieve maximum actomyosin interaction. Based on the crossbridge contraction theory (Huxley and Simmons, 1971), force generation and motion in striated muscle result from interactions between thin and thick filaments through the cyclical formation and rupture of the actomyosin bonds that act as crossbridges in the overlap region of the two filaments in sarcomeres. Previous studies have shown that there exists a relationship between actomyosin bonds and sarcomere length whereby sarcomere length decreases with an increase in actomyosin bonds and vice versa (Telley and Denoth, 2007). Thus, we speculate that if the sarcomere length remained the same in *sals* mutant myofibrils as in WT, the overlap between the myosin and shortened actin filaments would be severely reduced, completely impairing muscle function. Based on these considerations, we speculate that *sals* mutant myofibrils may compensate for this problem by adopting a shorter sarcomere length, thereby restoring a more optimal level of actomyosin interaction.

Moreover, we propose that the mechanical constraints placed on a muscle *in vivo* can explain the intriguing difference in sarcomere length that we observe in mutant *sals* muscles *in vivo* compared to those grown in culture. As we report, absence of SALS leads to 70% shortening of the sarcomeres in the myotubes in culture (Figure 1), but to only a 27% reduction in sarcomere length in muscles *in vivo* (Figures 3 and 4). Because the sarcomeres are presumably contracting under a much heavier load *in vivo* compared to myofibrils grown in culture, we reason that *sals* mutant sarcomeres are not able to shorten as much *in vivo* as they do in culture. We also note that such dramatic difference cannot be attributed to the age difference between muscles of 22 hr-old *sals* mutant embryos and those of ≥ 5 day-old *sals* mutant muscles in culture, since there is no difference in sarcomere length between WT embryonic and larval muscles.

In addition, *sals* mutant myofibrils grown in primary cultures showed an increase in sarcomere number, resulting in mutant myofibrils with a length similar to their WT counterparts. Here again, the increase in sarcomere number may reflect a compensatory mechanism intended to achieve a strength of contraction comparable to that of WT myofibrils. Indeed, shortened sarcomeres, which have reduced actomyosin compared to WT sarcomeres, may not be as efficient as a single contractile unit. Thus, the addition of more such sarcomeres to a myofibril might restore better functionality. This compensatory addition of

(J) Model of thin-filament assembly steps under conditions of either no SALS, normal SALS, or excess SALS. The final length of thin filaments is attained in a two-step process. Short thin filaments can form under no SALS conditions (step 1), whereas longer thin filaments are achieved only in the presence of SALS (step 2). However, excess SALS, depending on the timing and its dosage, can either disrupt sarcomere organization or increase thin-filament length within sarcomeres.

The scale bar is 30 μm in (A) for (A) and (B), 10 μm in (C) for (C)–(E), and 10 μm in (G) for (G)–(I).

sarcomeres probably also occurs in *sals* mutant myofibrils in vivo. Indeed, muscles of *sals* mutant larvae at 28–30 hr AEL had many more sarcomeres (~18 compared to 12 in age-matched controls). However, the muscle length was much shorter (only ~70% of their WT counterparts) at this stage, indicating that mutant muscles with shortened sarcomeres may grow much more slowly than in WT at the same stage. Moreover, from 28–30 hr AEL onward, *sals* mutant muscles were completely disrupted, and mutant animals eventually died. This is probably due to mechanical stresses placed on the muscle by other tissues during development. We speculate that the force generated by *sals* mutant muscles of a shorter size may not be strong enough to sustain these mechanical stresses in vivo, and the mutant animals died long before their muscles could achieve the same length as in WT. This is in contrast to the *sals* mutant muscle in culture, which is able to attain a final muscle length similar to WT controls while still maintaining normal striated morphology after being cultured for a long period of time, most likely due to the lack of the mechanical stresses present in the whole animal.

A Two-Step Model of the Thin-Filament Assembly Process

Thin filaments are still assembled in the absence of SALS, although their length is significantly shortened, indicating that SALS is not required for initial thin-filament assembly (Figures 1B and 4). However, SALS is absolutely required for thin filaments to attain a longer length, and we show that SALS promotes thin-filament lengthening from pointed ends (Figures 5 and 6). These data reveal a two-step process of thin-filament assembly in *Drosophila* larval muscles (Figure 7J). During step 1, short filaments are assembled, whereas during step 2, which depends on SALS activity, the filaments expand to their final lengths from their pointed ends (Figure 7J). *actin* RNAi presumably disrupts both thin-filament assembly steps. Thus, *actin* RNAi primary muscles contain both shortened sarcomeres that have thin filaments that fail to elongate and shortened myofibrils that fail to grow longitudinally through the addition of more sarcomeres, whose assembly presumably requires assembly of short thin filaments (step 1). In contrast, *sals* RNAi only disrupts the second elongation step, but it still allows the addition of short sarcomeres containing short thin filaments to preexisting myofibrils to attain normal myofibril length. A similar two-step process has also been implicated in myofibril assembly of the fly adult IFM (Mardahl-Dumesnil and Fowler, 2001). Although we are not yet able to efficiently disrupt SALS function to examine its role in IFM thin-filament assembly, SALS is most likely involved, because it is localized at the pointed ends of elongating thin filaments during IFM development (Figure 5).

Possible SALS Activity in Vertebrate Striated Muscle and Nonmuscle Cells

Studies on myofibrillogenesis in vertebrate striated muscles also suggest a similar two-step process in thin-filament assembly. For example, during early myofibrillogen-

esis in the chick cardiac myocytes, sarcomeres grow from ~1.5 μm to 1.8–2.5 μm , and their thin filaments elongate accordingly (Gregorio and Antin, 2000). Delayed assembly of Tmod at pointed end was thought to contribute to this elongation process (Gregorio et al., 1995). In addition, inhibition of Tmod activity in these cells causes excessive thin-filament elongation into H zones (Gregorio et al., 1995). These newly assembled filaments from uncapped pointed ends are unlikely to result from the sole modulation of the function of currently known proteins such as TM or cofilin, which maintain thin-filament length by stabilizing filaments and/or inhibiting their depolymerization from pointed ends (Littlefield and Fowler, 1998). Because these proteins only limit existing filament size, but do not contribute to actin assembly (Iwasa and Mullins, 2007), efficient pointed-end assembly is likely to involve a SALS-like activity.

SALS-like activity is unlikely to play a role in actin assembly in cellular processes that require actin filaments to turn over rapidly, such as protrusion of the leading edge of lamellipodia, where the pointed ends are the sites for rapid filament disassembly. However, it may be important for length specification of stable actin-filament structure that requires regulation of actin assembly from pointed ends, such as in hair cell rootlets of chick cochlea (Tilney and DeRosier, 1986). Thus, even though BLAST searches failed to identify any close SALS orthologs in vertebrates, functionally related proteins are likely to exist. There are several uncharacterized WH2-containing proteins present in human and mouse genomes (Paunola et al., 2002), and one or more of these may regulate actin-filament lengthening from pointed ends.

EXPERIMENTAL PROCEDURES

Drosophila Genetics

Drosophila strains used in this study were *Dmef2-Gal4* (Ranganavakulu et al., 1996); *UAS-GFPactin57B* (Roper et al., 2005); *TTG (TM3, Twi-Gal4, UAS-2EGFP, Ser)* and *twi^{D96}* (from Dr. A. Michelson); *P{PZ}tho[1]*, *PBac{WH}f07849* (Thibault et al., 2004); and *Df(3R)M-Kx1* (from the Bloomington *Drosophila* Stock Center). *w¹¹¹⁸* was used as a control strain. Excision of the piggyBac element from *PBac{WH}f07849* was done as described (Thibault et al., 2004).

Embryonic Primary Cell Cultures and Primary Cell RNAi

Embryonic primary cell cultures were established mainly as described (Bernstein et al., 1978). Cells were seeded and grown either in 384-well optically clear plates (Costar) (in Figure 1B) or in LabTek 8-well chamber coverglass slides (VWR) coated with human vitronectin (Chemicon) (Volk et al., 1990) (used for culturing of primary muscles shown in the insets of Figure 1B and in Figures 6 and 7), at $1.7\text{--}2.5 \times 10^5$ cells/cm². Mature primary muscles used for analyses were usually from 12-day cultures at 18°C or from 5-day cultures at 25°C or 29°C.

A detailed description of the establishment of the primary cell RNAi protocol will be described elsewhere. Briefly, the primary cells were isolated from postgastrula embryos (4–6 hr AEL) and were seeded in plates containing dsRNAs at around 4×10^4 cells per well. After 22 hr in serum-free M3 medium, additional serum-containing culture medium was added to bring the solution to a final concentration of 10% FCS. After an additional 11 days of culturing at 18°C, primary cells were directly fixed with 4% formaldehyde (Polyscience, Niles, USA). dsRNAs were prepared as described at <http://flyrnai.org/>. The oligos

for making dsRNAs used in this study can be found in the [Supplemental Data](#).

Molecular Biology, Germline Transformation, In Situ Hybridization, and Antibody Production
See the [Supplemental Data](#).

Actin-Binding Assays and Actin-Polymerization Assay

The GST pull-down assays, cosedimentation assays, and pyrene actin-polymerization assay were carried out as described (Martinez-Quiles et al., 2001). The actin assembly rate was measured as described (Pollard and Mooseker, 1981). Details can be found in the [Supplemental Data](#).

Immunofluorescence Microscopy and Image Analysis

Late embryos or larvae were dissected in Ca²⁺-free saline buffer (relaxing buffer) as described (Budnik et al., 2006). Myofibrils from dorsal longitudinal muscles of pupal and adult IFM were isolated as described (Mardahl-Dumesnil and Fowler, 2001). In general, dissected tissues and primary cells were fixed in 4% formaldehyde in relaxing buffer for 20–30 min, and the standard immunohistochemistry protocol was then followed (Budnik et al., 2006). The stained samples were analyzed on a Leica LSM NT confocal microscope. Primary antibodies used in this study can be found in the [Supplemental Data](#).

Analyses of myofibril features such as thin-filament length and sarcomere length were performed from deconvoluted images by using Leica confocal software TCS SP2. Thin-filament length was defined as half the distance between Tmod peaks or half the width of the phalloidin bands or the distance between Tmod and neighboring α -actinin peaks. Sarcomere length was defined as the distance between α -actinin bands or between midlines of the phalloidin bands.

Electron Microscopy

See the [Supplemental Data](#).

Supplemental Data

Supplemental Data include Supplemental Experimental Procedures, five figures, and movies and are available at <http://www.developmentalcell.com/cgi/content/full/13/6/828/DC1/>.

ACKNOWLEDGMENTS

We thank Drs. P. Beachy, J. Saide, W. Chia, A. Michelson, V. Fowler, H. Bellen, and D. Andrew, and the *Drosophila* Bloomington Stock Center for fly stocks and antibodies. We are also very grateful to R. Binari and C. Villalta for technical help, J. Ni for help in the production of SALS protein, A. Lebensohn for help in actin-binding assays, and A. Samsnova for help in data analysis of peristalsis movies. We also thank V. Fowler, B. Mathey-Prevot, C. Bakal, C. Pitsouli, and J. Zirin for critical comments on the manuscript. J.B. was supported by the Damon Runyon Cancer Research Foundation Fellowship DRG-1716-02. N.P. is an Investigator of the Howard Hughes Medical Institute.

Received: August 22, 2006

Revised: July 20, 2007

Accepted: October 4, 2007

Published: December 3, 2007

REFERENCES

Arber, S., Hunter, J., Ross, J., Hongo, M., Sansig, G., Borg, J., Perriard, J., Chien, K., and Caroni, P. (1997). MLP-deficient mice exhibit a disruption of cardiac cytoarchitectural organization, dilated cardiomyopathy, and heart failure. *Cell* 88, 393–403.

Bang, M., Li, X., Littlefield, R., Bremner, S., Thor, A., Knowlton, K., Lieber, R., and Chen, J. (2006). Nebulin-deficient mice exhibit shorter thin filament lengths and reduced contractile function in skeletal muscle. *J. Cell Biol.* 173, 905–916.

Bear, J., Svitkina, T., Krause, M., Schafer, D., Loureiro, J., Strasser, G., Maly, I., Chaga, O., Cooper, J., Borisy, G., et al. (2002). Antagonism between Ena/VASP proteins and actin filament capping regulates fibroblast motility. *Cell* 109, 509–521.

Bernstein, S., Fyrberg, E., and Donady, J. (1978). Isolation and partial characterization of *Drosophila* myoblasts from primary cultures of embryonic cells. *J. Cell Biol.* 78, 856–865.

Budnik, V., Gorczyca, M., and Prokop, A. (2006). Selected methods for the anatomical study of *Drosophila* embryonic and larval neuromuscular junctions. *Int. Rev. Neurobiol.* 75, 323–365.

Burkholder, T., Fingado, B., Baron, S., and Lieber, R. (1994). Relationship between muscle fiber types and sizes and muscle architectural properties in the mouse hindlimb. *J. Morphol.* 221, 177–190.

Chereau, D., Kerff, F., Graceffa, P., Grabarek, Z., Langsetmo, K., and Dominguez, R. (2005). Actin-bound structures of Wiskott-Aldrich syndrome protein (WASP)-homology domain 2 and the implications for filament assembly. *Proc. Natl. Acad. Sci. USA* 102, 16644–16649.

Dix, D., and Eisenberg, B. (1990). Myosin mRNA accumulation and myofibrillogenesis at the myotendinous junction of stretched muscle fibers. *J. Cell Biol.* 111, 1885–1894.

Fischer, R.S., and Fowler, V.M. (2003). Tropomodulins: life at the slow end. *Trends in Cell Biology* 13, 593–601.

Granzier, H., Akster, H., and Ter Keurs, H. (1991). Effect of thin filament length on the force-sarcomere length relation to skeletal muscle. *Am. J. Physiol. Cell Physiol.* 260, C1060–C1070.

Gregorio, C., and Antin, P. (2000). To the heart of myofibril assembly. *Trends Cell Biol.* 10, 355–362.

Gregorio, C., Weber, A., Bondad, M., Pennise, C., and Fowler, V. (1995). Requirement of pointed-end capping by tropomodulin to maintain actin filament length in embryonic chick cardiac myocytes. *Nature* 377, 83–86.

Haas, J. (1950). Cytoplasmic growth in the muscle fibers of larvae of *Drosophila melanogaster*. *Growth* 14, 277–294.

Huxley, A., and Simmons, R. (1971). Proposed mechanism of force generation in striated muscle. *Nature* 233, 533–538.

Iwasa, J., and Mullins, R. (2007). Spatial and temporal relationships between actin-filament nucleation, capping, and disassembly. *Curr. Biol.* 17, 395–406.

Littlefield, R., and Fowler, V. (1998). Defining actin filament length in striated muscle: rulers and caps or dynamic stability? *Annu. Rev. Cell Dev. Biol.* 14, 487–525.

Littlefield, R., Almenar-Queral, A., and Fowler, V. (2001). Actin dynamics at pointed ends regulates thin filament length in striated muscle. *Nat. Cell Biol.* 3, 544–551.

Ma, Y., Creanga, A., Lum, L., and Beachy, P. (2006). Prevalence of off-target effects in *Drosophila* RNA interference screens. *Nature* 443, 359–363.

Machado, C., Sunkel, C., and Andrew, D. (1998). Human autoantibodies reveal titin as a chromosomal protein. *J. Cell Biol.* 141, 321–333.

Mardahl-Dumesnil, M., and Fowler, V. (2001). Thin filaments elongate from their pointed ends during myofibril assembly in *Drosophila* indirect flight muscle. *J. Cell Biol.* 155, 1043–1053.

Martinez-Quiles, N., Rohatgi, R., Anton, M., Medina, M., Saville, S., Miki, H., Yamaguchi, H., Takenawa, T., Hartwig, J., Geha, R., et al. (2001). WIP regulates N-WASP-mediated actin polymerization and filopodium formation. *Nat. Cell Biol.* 3, 484–491.

McElhinny, A., Schwach, C., Valichnac, M., Mount-Patrick, S., and Gregorio, C. (2005). Nebulin regulates the assembly and lengths of the thin filaments in striated muscle. *J. Cell Biol.* 170, 947–957.

Mohri, K., Ono, K., Yu, R., Yamashiro, S., and Ono, S. (2006). Enhancement of actin-depolymerizing factor/cofilin-dependent actin disassembly by actin-interacting protein 1 is required for organized actin

- filament assembly in the *Caenorhabditis elegans* body wall muscle. *Mol. Biol. Cell* **17**, 2190–2199.
- Newman, S., and Wright, T. (1981). A histological and ultrastructural analysis of developmental defects produced by the mutation, *lethal(1)-mysospheroid*, in *Drosophila melanogaster*. *Dev. Biol.* **86**, 393–402.
- Page, S., and Huxley, H. (1963). Filament lengths in striated muscle. *J. Cell Biol.* **19**, 369–390.
- Paunola, E., Mattila, P., and Lappalainen, P. (2002). WH2 domain: a small, versatile adaptor for actin monomers. *FEBS Lett.* **513**, 92–97.
- Pollard, T., and Mooseker, M. (1981). Direct measurement of actin polymerization rate constants by electron microscopy of actin filaments nucleated by isolated microvillus cores. *J. Cell Biol.* **88**, 654–659.
- Pollard, T., Blanchoin, L., and Mullins, R. (2000). Molecular mechanisms controlling actin filament dynamics in nonmuscle cells. *Annu. Rev. Biophys. Biomol. Struct.* **29**, 545–576.
- Ranganavakulu, G., Schulz, R., and Olson, E. (1996). *Wingless* induces *nautilus* expression in the ventral mesoderm of the *Drosophila* embryo. *Dev. Biol.* **176**, 143–148.
- Reedy, M.C., and Beall, C. (1993). Ultrastructure of developing flight muscle in *Drosophila*. I. Assembly of myofibrils. *Dev. Biol.* **160**, 443–465.
- Roper, K., Mau, Y., and Brown, N. (2005). Contribution of sequence variation in *Drosophila* actins to their incorporation into actin-based structures in vivo. *J. Cell Sci.* **118**, 3937–3948.
- Sussman, M., Baqué, S., Uhm, C., Daniels, M., Price, R., Simpson, D., Terracio, L., and Kedes, L. (1998). Altered expression of tropomodulin in cardiomyocytes disrupts the sarcomeric structure of myofibrils. *Circ. Res.* **82**, 94–105.
- Sussman, M., Welch, S., Gude, N., Khoury, P., Daniels, S., Kirkpatrick, D., Walsh, R., Price, R., Lim, H., and Molkentin, J. (1999). Pathogenesis of dilated cardiomyopathy: molecular, structural, and population analyses in tropomodulin-overexpressing transgenic mice. *Am. J. Pathol.* **155**, 2101–2113.
- Telley, I., and Denoth, J. (2007). Sarcomere dynamics during muscular contraction and their implications to muscle function. *J. Muscle Res. Cell Motil.* **28**, 89–104.
- Thibault, S., Singer, M., Wiyazaki, W., Milash, B., Dompe, N., Singh, C., Buchholz, R., Demsky, M., Fawcett, R., Francis-Lang, H., et al. (2004). A complementary transposon tool kit for *Drosophila melanogaster* using P and piggyBac. *Nat. Genet.* **36**, 283–287.
- Tilney, L., and DeRosier, D. (1986). Actin filaments, stereocilia, and hair cells of the bird cochlea. IV. How the actin filaments become organized in developing stereocilia and in the cuticular plate. *Dev. Biol.* **116**, 119–129.
- Volk, T., Fessler, L., and Fessler, J. (1990). A role for integrin in the formation of sarcomeric cytoarchitecture. *Cell* **63**, 525–536.
- Williams, P., and Goldspink, G. (1971). Longitudinal growth of striated muscle fibers. *J. Cell Sci.* **9**, 751–767.
- Witt, C., Burkart, C., Labeit, D., MaNabb, M., Wu, Y., Granzier, H., and Labeit, S. (2006). Nebulin regulates thin filament length, contractility, and Z-disk structure in vivo. *EMBO J.* **25**, 3843–3855.
- Yamaguchi, M., Robson, R., Stromer, M., Dahl, D., and Oda, T. (1978). Actin filaments form the backbone of nemaline myopathy rods. *Nature* **271**, 265–267.
- Yin, H., Hartwig, J., Maruyama, K., and Stosel, T. (1981). Ca²⁺ control of actin filament length. Effects of macrophage gelsolin on actin polymerization. *J. Biol. Chem.* **256**, 9693–9697.
- Zhukarev, V., Sanger, J., Sanger, J., Goldman, Y., and Shuman, H. (1997). Distribution and orientation of rhodamine-phalloidin bound to thin filaments in skeletal and cardiac myofibrils. *Cell Motil. Cytoskeleton* **37**, 363–377.
- Zigmond, S., Evangelista, M., Boone, C., Yang, C., Dar, A., Sicheri, F., Forkey, J., and Pring, M. (2003). Formin leaky cap allows elongation in the presence of tight capping proteins. *Curr. Biol.* **13**, 1820–1823.